Phase Retrieval Camera for Testing NGST Optics

Andrew E. Lowman*, David C. Redding, Scott A. Basinger, David Cohen,
Jessica A. Faust, Joseph J. Green, Catherine M. Ohara, Fang Shi

Jet Propulsion Laboratory (JPL), California Institute of Technology, Pasadena, CA 91109

ABSTRACT

The NGST Phase Retrieval Camera (PRC) is a portable wavefront sensor useful for optical testing in high-vibration environments. The PRC uses focus-diverse phase retrieval to measure the wavefront propagating from the optical component or system under test. Phase retrieval from focal plane images is less sensitive to jitter than standard pupil plane interferometric measurements; the PRC's performance is further enhanced by using a high-speed shutter to freeze out seeing and jitter along with a reference camera to maintain the correct boresight in defocused images. The PRC hardware was developed using components similar to those in NGST's Wavefront Control Testbed (WCT), while the PRC software was derived from the testbed's extensive software infrastructure. Primary applications of the PRC are testing and experimenting with NGST technology demonstrator mirrors, along with exploring other wavefront sensing and control problems not easily studied using WCT. An overview of the hardware and testing results will be presented.

Keywords: NGST, optical testing, wavefront sensing, dispersed fringe sensor, phase retrieval

1. INTRODUCTION

The Wavefront Control Testbed (WCT) was built to explore and demonstrate critical wavefront sensing and control technologies needed for the Next Generation Space Telescope (NGST).[1] WCT currently consists of a source module, telescope simulator module containing alternate paths to either a small deformable mirror (DM) or a small cluster of segmented, a set of relay optics to image the segmented mirror onto a larger DM, and a wavefront sensor formed by combining a scientific camera with a motorized translation stage.[2] An image-based wavefront sensing approach called focus-diverse phase retrieval is used to measure the wavefront before and after correction with the large DM. One important property of phase retrieval is its low sensitivity to jitter. Since the blurring occurs laterally in an image plane and defocused images are spread over many pixels, the degradation is graceful, and useful measurements may still be obtained even with several pixels of jitter.

The NGST mirror technology programs have demonstrated the need for jitter-insensitive instruments. Both the NGST Mirror System Demonstator (NMSD) and Advanced Mirror System Demonstrator (AMSD) programs include cryogenic testing at Marshall Space Flight Center's X-Ray Calibration Facility (XRCF). The XRCF was designed for testing of Chandra optics and does not include active vibration isolation. Larger facilities that will be used for NGST mirror and system testing may also present a challenge for optical testing. Conventional interferometers cannot handle the high jitter levels present in the XRCF. Specialized simultaneous-frame interferometers were procured for this testing, but we also constructed a phase retrieval based instrument, called the Phase Retrieval Camera (PRC), to exploit the properties of image-based wavefront sensing.

The PRC is sized to fit anywhere a conventional interferometer would normally be used. Commercial off-the-shelf parts were used wherever possible, and the hardware design and extensive software infrastructure of WCT were reused with small modifications for this task. Besides NGST technology testing, the PRC is useful for general phase retrieval experiments outside WCT, DM testing, and early experience sensing and controlling NGST primary mirror optics. This paper provides an overview of the PRC design and performance; additional details can be found in reference (3).

* Contact: Andrew.E.Lowman@jpl.nasa.gov; phone 1 818 354 0526; Jet Propulsion Laboratory, M/S 306-451, 4800 Oak Grove Dr, Pasadena, CA, USA 91109-8099

2. BACKGROUND

Several methods fall under the heading of image-based wavefront sensing. Phase diversity uses an extended object and must simultaneously estimate both the wavefront and the object (if not known *a priori*). Phase retrieval uses a point source, which greatly simplifies processing. The specific technique used by the PRC is focus-diverse phase retrieval. Images taken with different amounts of defocus are processed together to yield a unique wavefront measurement. Calibrating the static aberrations of the PRC's optics and any auxiliary optics allows us to estimate the true wavefront of the optical component or system under test.

The specific calculation utilized is the Modified Gerchberg-Saxton (MGS) algorithm.[4] As depicted in Figure 1, this iterative Fourier transform technique computes the unknown wavefront phase by applying real data as a boundary condition in both the spatial and Fourier domains, with many iterations used to obtain convergence. A random phase is used as a starting point. Defocused images provide the data used in the spatial domain, while a pupil image is used to provide the amplitude data applied in the Fourier domain. Θ_{DIVx} corresponds to the phase due to each focus shift, while Θ_0 corresponds to the residual wavefront of the optical system. A unique solution is found by periodically replacing the estimated wavefront phase for each defocused image with a joint estimate based on the solutions found for multiple defocused images. Unwrapping is performed as needed if the wavefront exceeds one wave, since each phase solution is modulo 2π.

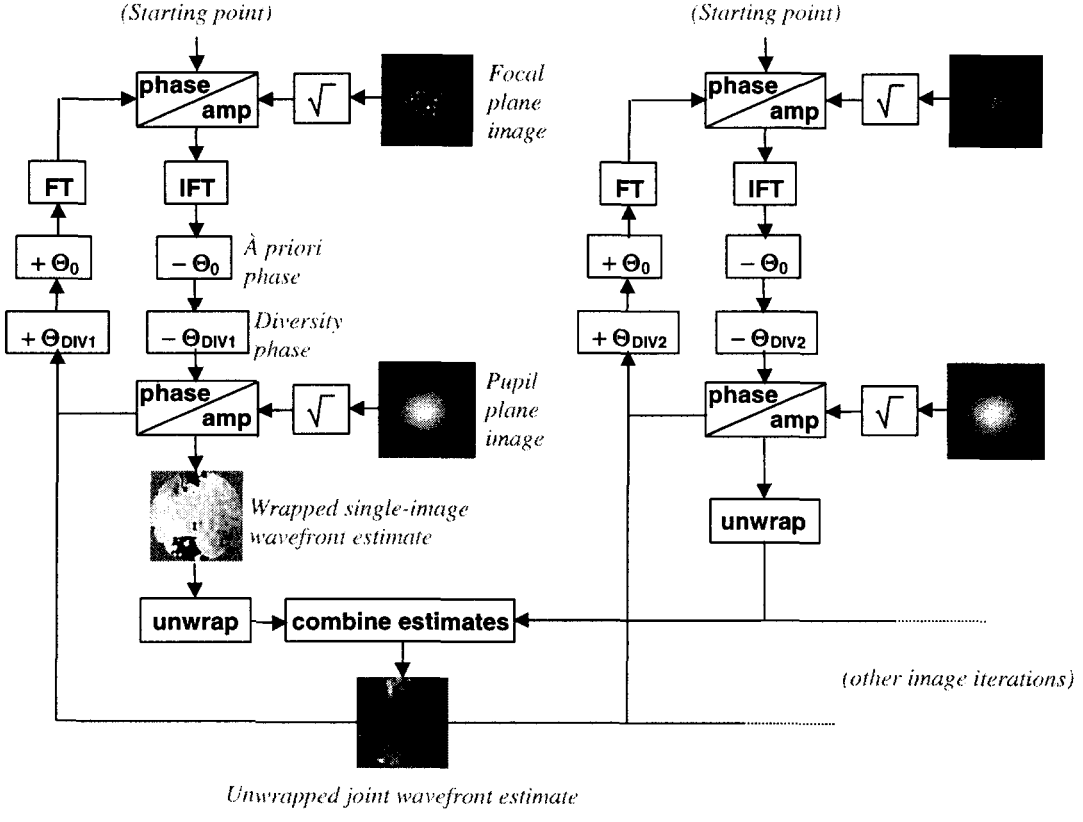

Figure 1. Modified Gerchberg-Saxton algorithm.

3. HARDWARE DESCRIPTION

The PRC consists of a source module, single-mode fiber, sensor module, diverger lens or other auxiliary optics, electronics rack, and computers. A layout of the optomechanical hardware is shown in Figure 2.

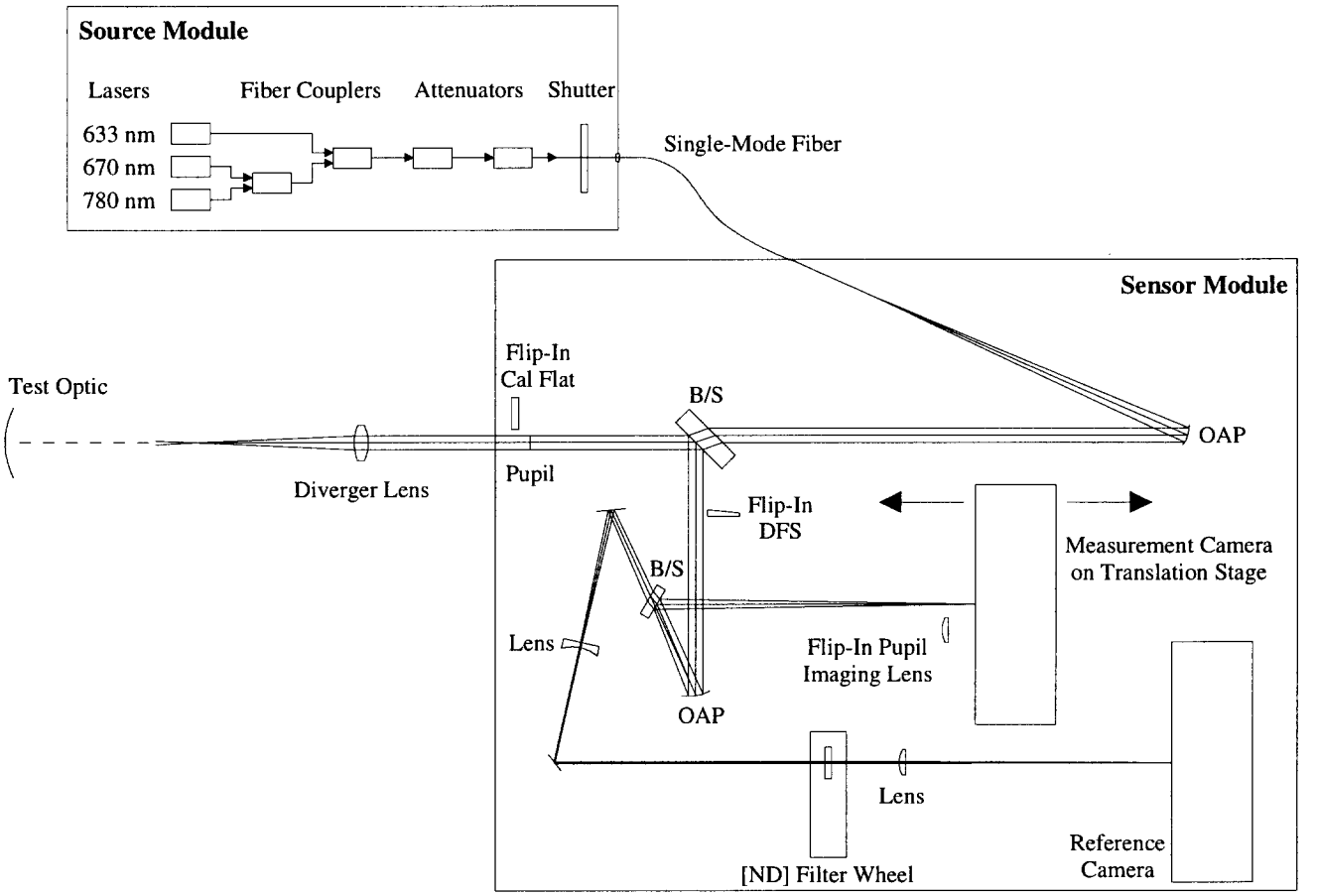

Figure 2. PRC layout

1. Sensor Module

The hardware used specifically for the phase retrieval calculation consists of a science grade camera, a motorized translation stage, and a lens on a flip-in mechanism. The science grade CCD minimizes the impact of detector noise on the wavefront calculation. The motorized translation stage enables use of arbitrary defocus amounts for different images. The flip-in lens is positioned to image the pupil onto the CCD.

The other primary purpose of the sensor module is to minimize and correct for the effects of image jitter. The minimum practical exposure time of the measurement camera is 0.1 sec; shorter exposures will have non-uniform illumination due to the opening and closing time of the shutter blades. Measurement of the XRCF showed PV jitter of 120 μm (13 pixels) on faster time scales than this.[5] To freeze out the jitter, a high speed shutter is used, providing exposure times down to 0.3 msec. To get high signal-to-noise ratio (SNR) images in such a short time, a laser diode source is used. (Phase retrieval works best with a narrowband source, so a laser is desirable for that reason as well.) Arbitrarily centering the images used in the MGS algorithm can introduce artifacts into the wavefront estimate, so an identical camera is used as a

reference to provide an in-focus image to monitor changes in the boresight as the measurement camera is defocused. Jitter in the test optic will be common path between the reference and measurement cameras, allowing shift-and-add processing of the measurement camera images. The reference beam is magnified by a factor of 4 to improve centroiding accuracy. The reference camera can also be used to identify and remove from processing those extreme cases where image motion is significant over 0.3 msec.

The PRC optics consist of high quality (λ/20 PV) fold mirrors, beamsplitters, and off-axis paraboloidal mirrors (OAP's). An aperture (pupil) is positioned at the front focal point of the second OAP to make the system telecentric in image space. Telecentricity ensures that the diffraction propagator applied to defocused images in the MGS algorithm will not introduce a scale change in the Fourier domain data arrays for different defocus positions. If the exit pupil were not located far from the image plane, significant scale changes would appear and interpolation of the data arrays would be required. A flat mirror on a flip-in mechanism resides near the pupil, providing easy calibration of the PRC's internal wavefront error.

The PRC will also include another device for wavefront sensing, a dispersed fringe sensor (DFS), which measures piston in a segmented optic or optical system.[6] The DFS consists of a grism on a flip-in mechanism. A white light source will be used in this mode. The grism disperses the light and effectively modulates the fixed wavefront piston with a varying wavelength. The amount of piston is related to the period of the resulting fringes. Piston can also be measured using phase retrieval measurements taken with different wavelengths.

2. Auxiliary Optics

Auxiliary optics, such as a diverger or null lenses, can be mounted on a small attachment to the sensor module. These are used to match the small collimated PRC output beam to the test optic or optical system. These optics also must image the test optic or exit pupil onto the entrance pupil of the PRC, to keep the combined system telecentric in image space.

3. Source Module

Illumination for the PRC is provided by a source module containing lasers, attenuators, the input from an external white light source, and the high speed shutter. (Initially, the shutter was mounted inside the sensor module, but there were concerns about it as a source of jitter.) One laser diode is adequate for phase retrieval, but using multiple lasers with different wavelengths will allow measurement of piston via phase retrieval. Two inline fiber attenuators control the source flux. Significant attenuation is needed when the measurement camera is in focus; however, as the camera is defocused and the light is spread over many pixels, the source signal is increased to maintain a high SNR in the image. The external white light source contains a Xenon lamp and optics to image the beam into a single-mode fiber. A motorized filter wheel contains narrowband filters for calibrating the DFS.

4. Electronics, Computers, and Software

The sensor module is connected to a large rack holding the source module, electronics, and computers. The hardware is driven by a personal computer containing data acquisition and frame grabber boards. Numerical computations are done in a standalone configuration using a Beowulf system consisting of two rack-mounted PC's running Linux and distributed processing software. Other systems can be used via the Internet.

The software element consists of two components: control software for the PC driving the hardware; and the Executive software for remotely controlling the hardware and running experiments/performing measurements. Both are derived from software written for WCT.[7] The control program allows both local commanding via a graphical user interface or remote commanding via the Internet. The actual measurement/experimentation work is performed using the PRC Executive. This program allows the user to define the sequence of events needed to make a measurement and sends commands to the control computer over a local area network or the Internet to drive specific hardware items and receive image data.

4. RESULTS

A representative data series is shown in Figure 3, taken using an external flat mirror as the test optic. Defocus values are (A) -15 mm; (B) -10 mm; (C) +10 mm; and (D) +15 mm. The pupil image is (E). No auxiliary optics were used to image the test flat onto the internal aperture (pupil); consequently, some diffraction rings can be seen at the edge of the pupil image. (F) shows the in-focus image, though this is generally not used in the MGS algorithm because it adds more noise than information.

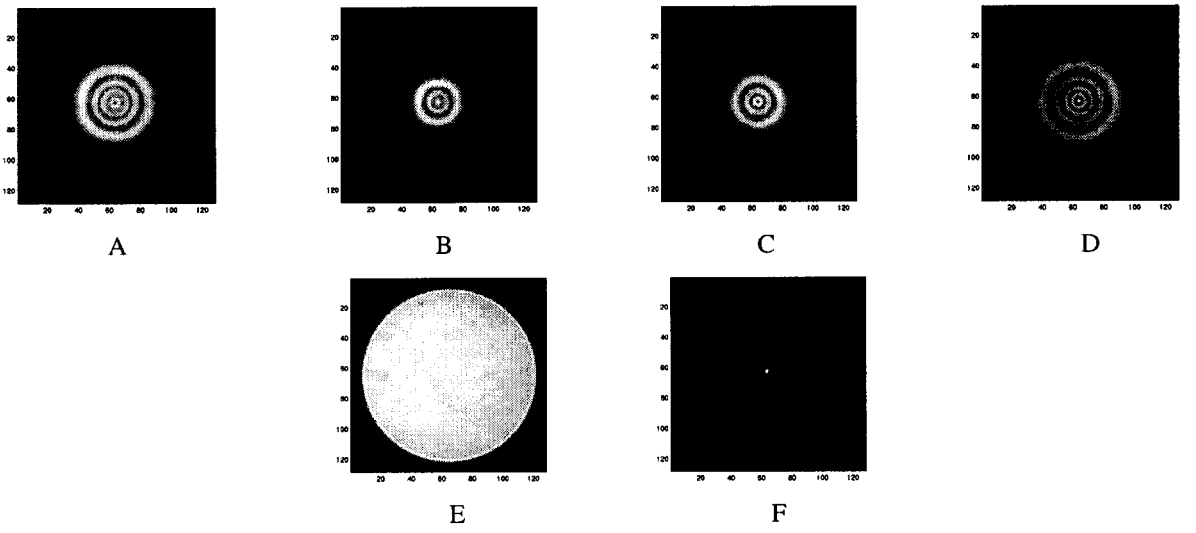

Figure 3. Data taken with external flat mirror

The resulting wavefront from this data in is shown in Figure 4. (A) is the result of the MGS processing; PV is 121.9 nm, RMS 27.9 nm. (B) has power removed after Zernikes were fit to the wavefront in (A); PV is 39.6 nm, RMS 5.9 nm. The granularity in the maps is a result of a relatively small (128 X 128) array size used for processing this case. Better lateral resolution can be obtained by using larger arrays, at the expense of processing time.

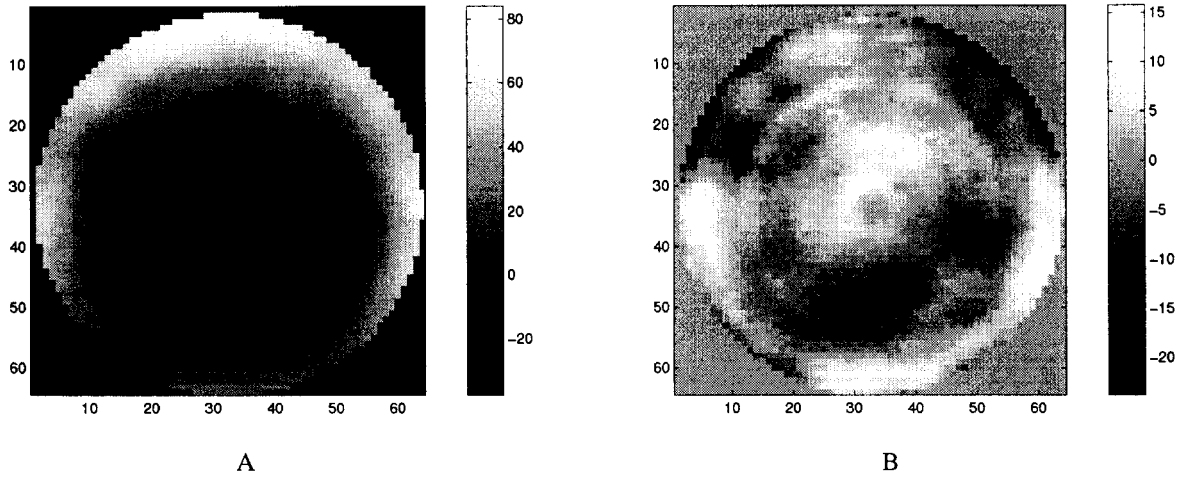

Figure 4. Measured wavefront (A); with power removed (B)

A measurement of the internal aberrations of the PRC, taken using the internal calibration flat, is shown in Figure 5. Wavefront error is on the order of 60 nm PV, 6 nm RMS (or λ/100 using λ=632.8nm). This wavefront can be stored and subtracted from other measurements to yield more accurate results. (The accuracy of this measurement is limited by the accuracy of the MGS algorithm, as well as any errors in the calibration flat.)

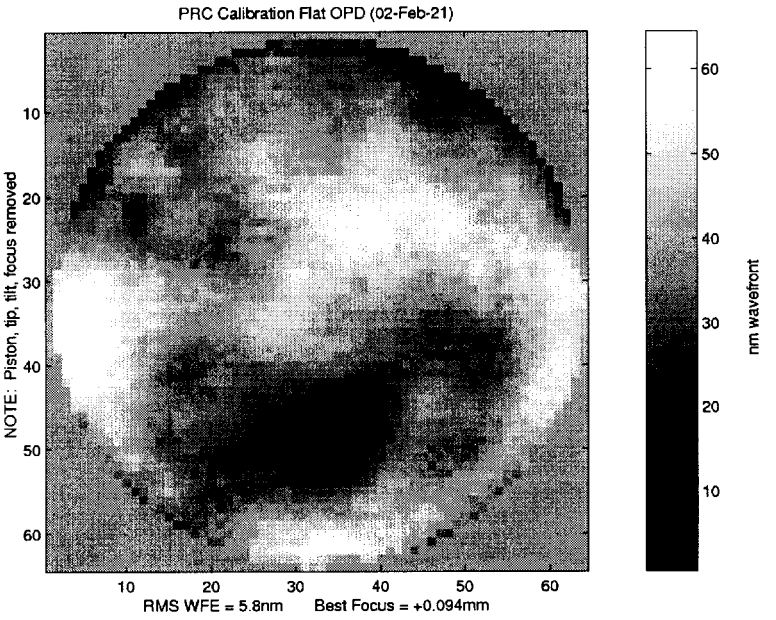

Figure 5. Internal PRC aberrations.

Multiple data sets taken with the calibration flat have shown repeatability on the order of λ/235 (λ=632.8nm). Figure 6(A) shows the standard deviation of 10 measurements (RMS = 2.7 nm). Figure 6(B) shows the 3rd and 5th order aberration component, found by fitting 15 Zernikes (RMS = 2.0 nm). A 256X256 array size was used in the processing, giving twice the lateral resolution shown in Figures 4 and 5.

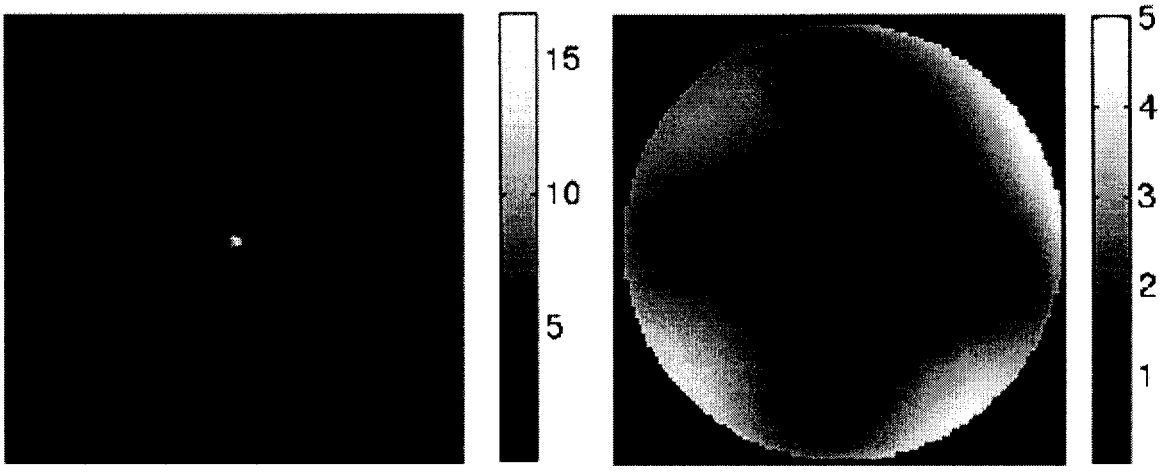

Figure 6. Repeatability of PRC measurements: (A) raw data; (B) low order aberration component

An experiment was conducted to compare image-based wavefront sensing in general with interferometry. Differential measurements were used on a fiducialized part to remove the internal instrument aberrations from the PRC and a commercial interferometer. The wavefront measurements agreed to within 5.7 nm ($\lambda/118$); when measurement repeatabilities were taken into account, they agreed to within 1.5 nm ($\lambda/450$). See reference (8) for further details.

5. CONCLUSION

The extensive experience and infrastructure of NGST's wavefront control testbed were leveraged to create the PRC, a portable, self-contained wavefront sensor useful for optical testing and additional image-based wavefront sensing experimentation. The instrument is designed to give good performance in the presence of high levels of jitter, using a high speed shutter and reference camera to minimize the impact of jitter that exceeds what phase retrieval can tolerate. Initial results show good repeatability, low internal jitter, and low static aberrations in the system.

6. ACKNOWLEDGMENTS

The authors wish to thank Randy Hein, Yuri Beregovski, and Hiroshi Kadogawa for support in mechanical design, fabrication, assembly, and alignment of the PRC at JPL.

Research described in this paper was carried out at the Jet Propulsion Laboratory, California Institute of Technology, under contract with the National Aeronautics and Space Administration.

7. REFERENCES

1. D. C. Redding, S. A. Basinger, C. W. Bowers, R. Burg, L. A. Burns, D. Cohen, B. H. Dean, J. J. Green, A. E. Lowman, C. M. Ohara, F. Shi, "Next Generation Space Telescope wavefront sensing and control," Proc. Soc. Photo-Opt. Instrum. Eng. **4850-49** (Waikoloa, HI, Aug 2002).
2. P. Petrone III, S. A. Basinger, C. W. Bowers, D. Cohen, L. A. Burns, A. Chu, P. S. Davila, P. Dogota, B. H. Dean, J. J. Green, K. Ha, W. L. Hayden, D. J. Lindler, A. E. Lowman, C. M. Ohara, D. C. Redding, F. Shi, M. E. Wilson, B. J. Zukowski, "Optical design and performance of the NGST wavefront control testbed," Proc. Soc. Photo-Opt. Instrum. Eng. **4850-55** (Waikoloa, HI, Aug 2002).
3. J. A. Faust, A. E. Lowman, D. C. Redding, S. A. Basinger, D. Cohen, J. J. Green, C. M. Ohara, F. Shi, "NGST phase retrieval camera design and experiment details," Proc. Soc. Photo-Opt. Instrum. Eng. **4850-61** (Waikoloa, HI, Aug 2002).
4. R. W. Gerchberg and W. O. Saxton, "A practical algorithm for the determination of phase from image and diffraction plane pictures," Optik **35**, 237-246 (1972).
5. M. Fitzmaurice, T. Norton, P. Petrone III, J. Schott, "Results of optical jitter tests at the MSFC X-Ray Calibration Facility," internal Goddard Space Flight Center report (25 Oct 2000).
6. F. Shi, D. C. Redding, A. E. Lowman, C. W. Bowers, L. A. Burns, P. Petrone III, C. M. Ohara, S. A. Basinger, "Segmented mirror coarse phasing with a dispersed fringe sensor: experiments on NGST's wavefront control testbed," Proc. Soc. Photo-Opt. Instrum. Eng. **4850-51** (Waikoloa, HI, Aug 2002).
7. S. A. Basinger, D. C. Redding, F. Shi, D. Cohen, J. J. Green, C. M. Ohara, A. E. Lowman, L. A. Burns, "Wavefront sensing and control software for a segmented space telescope," Proc. Soc. Photo-Opt. Instrum. Eng. **4850-56** (Waikoloa, HI, Aug 2002).
8. J. J. Green, D. C. Redding, Y. Beregovski, A. E. Lowman, C. M. Ohara, "Interferometric validation of image-based wavefront sensing for NGST," Proc. Soc. Photo-Opt. Instrum. Eng. **4850-53** (Waikoloa, HI, Aug 2002).